AMERICAN SOCIETY FOR MICROBIOLOGY | Infection and Immunity®

BACTERIAL INFECTIONS

Contribution of Active Iron Uptake to *Acinetobacter baumannii* Pathogenicity

Federica Runci,[a] Valentina Gentile,[a] Emanuela Frangipani,[a]* Giordano Rampioni,[a] Livia Leoni,[a] Massimiliano Lucidi,[a,b] Daniela Visaggio,[a] Greg Harris,[c] Wangxue Chen,[c] Julia Stahl,[d] Beate Averhoff,[d] Paolo Visca[a]

[a]Department of Science, Roma Tre University, Rome, Italy
[b]Department of Engineering, Roma Tre University, Rome, Italy
[c]Human Health Therapeutics, National Research Council Canada, Ottawa, Ontario, Canada
[d]Department of Molecular Microbiology and Bioenergetics, Institute of Molecular Biosciences, Goethe University, Frankfurt, Germany

ABSTRACT *Acinetobacter baumannii* is an important nosocomial pathogen. Mechanisms that allow *A. baumannii* to cause human infection are still poorly understood. Iron is an essential nutrient for bacterial growth *in vivo*, and the multiplicity of iron uptake systems in *A. baumannii* suggests that iron acquisition contributes to the ability of *A. baumannii* to cause infection. In Gram-negative bacteria, active transport of ferrisiderophores and heme relies on the conserved TonB-ExbB-ExbD energy-transducing complex, while active uptake of ferrous iron is mediated by the Feo system. The *A. baumannii* genome invariably contains three *tonB* genes (*tonB1*, *tonB2*, and *tonB3*), whose role in iron uptake is poorly understood. Here, we generated *A. baumannii* mutants with knockout mutations in the *feo* and/or *tonB* gene. We report that *tonB3* is essential for *A. baumannii* growth under iron-limiting conditions, whereas *tonB1*, *tonB2*, and *feoB* appear to be dispensable for ferric iron uptake. *tonB3* deletion resulted in reduced intracellular iron content despite siderophore overproduction, supporting a key role of TonB3 in iron uptake. In contrast to the case for *tonB1* and *tonB2*, the promoters of *tonB3* and *feo* contain functional Fur boxes and are upregulated in iron-poor media. Both TonB3 and Feo systems are required for growth in complement-free human serum and contribute to resistance to the bactericidal activity of normal human serum, but only TonB3 appears to be essential for virulence in insect and mouse models of infection. Our findings highlight a central role of the TonB3 system for *A. baumannii* pathogenicity. Hence, TonB3 represents a promising target for novel antibacterial therapies and for the generation of attenuated vaccine strains.

KEYWORDS *Acinetobacter baumannii*, drug targets, iron uptake, TonB, vaccine, virulence

Over the last 20 years *Acinetobacter baumannii* has emerged as one of the most dreaded opportunistic pathogens in hospitals, being responsible for local and systemic infections, especially in immunocompromised and severely ill patients (1). While the genetic and functional basis of multidrug resistance in *A. baumannii* clinical isolates is matter of intensive research, the mechanisms of *A. baumannii* pathogenicity are still poorly understood.

Iron (Fe) is an essential nutrient for all living organisms, since it is required as a cofactor for several enzymes, such as those implicated in electron transport and in amino acid and DNA biosynthesis (2, 3). In aerobic environments, iron exists in the oxidized ferric form [Fe(III)], which aggregates in insoluble oxy-hydroxy polymers. Conversely, in anaerobic and/or reducing environments, the prevalent iron species is the more soluble ferrous form [Fe(II)].

Citation Runci F, Gentile V, Frangipani E, Rampioni G, Leoni L, Lucidi M, Visaggio D, Harris G, Chen W, Stahl J, Averhoff B, Visca P. 2019. Contribution of active iron uptake to *Acinetobacter baumannii* pathogenicity. Infect Immun 87:e00755-18. https://doi.org/10.1128/IAI.00755-18.

Editor Andreas J. Bäumler, University of California, Davis

Address correspondence to Paolo Visca, paolo.visca@uniroma3.it.

* Present address: Emanuela Frangipani, Department of Biomolecular Sciences, University of Urbino Carlo Bo, Urbino, Italy.

Received 5 October 2018
Returned for modification 31 October 2018
Accepted 25 January 2019
Accepted manuscript posted online 4 February 2019
Published 25 March 2019

It has been postulated that the ability to acquire iron from the environment contributes to *A. baumannii* pathobiology and virulence (4–6). Upon entry into the human host, *A. baumannii* is faced with the low level of free iron imposed by the hypoferremic response and by the presence of high-affinity iron-binding proteins (e.g., transferrin and lactoferrin) (7). To counteract iron starvation, *A. baumannii* has developed several iron acquisition strategies, such as the production of different siderophores which are variably present in different strains and likely account for Fe(III) scavenging from different sources (8). Production of siderophores is stimulated under iron-limiting conditions and repressed when sufficient iron is present. The Fur (ferric uptake regulator) repressor protein acts as the master regulator of iron homeostasis; in bacteria containing sufficient iron levels, the Fur-Fe(II) complex blocks transcription arising from Fur-controlled promoters, which conversely are transcribed during iron starvation due to detachment of apo-Fur from iron-repressible promoters (9).

In Gram-negative bacteria, Feo is the main system for Fe(II) uptake (10), and it consists of three proteins encoded by the *feo* operon: FeoA, a small cytosolic protein with still-unknown functions; FeoB, a large protein involved in active translocation of Fe(II) across the cytoplasmic membrane with a cytosolic N-terminal G-protein domain and a C-terminal integral inner membrane domain; and FeoC, a small cytosolic protein likely acting as transcriptional repressor (11).

Bacterial systems involved in Fe(III) acquisition (via either siderophores or heme) require the TonB energy transducing machinery, consisting of the TonB-ExbB-ExbD protein complex (12). This complex transduces the proton motive force (PMF) of the cytoplasmic membrane into energy required for high-affinity active transport of Fe(III)-loaded carriers across outer membrane transporter proteins into the periplasmic space (13). Structurally, TonB consists of a short hydrophobic N-terminal transmembrane domain associated with ExbB and ExbD proteins, a proline-rich linker domain and a C-terminal domain interacting with a variety of the outer membrane transporters (12, 14). Up to 21 putative TonB-dependent outer membrane transporter genes have been identified or predicted in *A. baumannii* genomes, most often associated with putative or confirmed ferri-siderophore and heme uptake genes (8). TonB-dependent transporter proteins are all characterized by a short conserved signature at the N terminus called TonB box. Once TonB proficiently interacts with the TonB box of an outer membrane transporter, translocation of the transporter-bound ligand into the periplasmic space occurs (14–16).

Although the TonB and Feo systems have extensively been studied in prototypic Gram-negative bacteria, including *Escherichia coli* and *Pseudomonas aeruginosa* (16–21), knowledge about these systems in *A. baumannii* is still limited. Three genes coding for TonB proteins have been identified in the chromosome of the *A. baumannii* type strain ATCC 19606^T, namely, *tonB1*, *tonB2*, and *tonB3* (6). The *tonB1* and *tonB3* genes are components of typical *tonB-exbB-exbD* operons, while *tonB2* is monocistronic (Fig. 1). In a seminal work by Luis Actis' group, insertional mutagenesis suggested a modest contribution of *tonB1* and *tonB2* to bacterial growth under low-iron conditions (6). Until now, no data on the role of *tonB3* in *A. baumannii* iron uptake and virulence have been available, mainly due to failure in generating *tonB3* knockouts (6).

To gain further insight into the contribution of the TonB and Feo system to *A. baumannii* pathogenicity, we generated mutants with single and multiple mutations in the *A. baumannii tonB* and/or *feo* gene and tested them in insect and mammalian models of acute infection. Marked differences in the individual contributions of TonB and Feo systems to iron acquisition by *A. baumannii* were observed, with TonB3 being crucial for iron acquisition and pathogenicity. These findings encourage future exploitation of TonB3 druggability and pave the way for the generation of attenuated *A. baumannii* vaccine strains.

RESULTS

TonB3 is essential for *A. baumannii* growth under iron-limiting conditions. To assess the contributions of the TonB and Feo systems to iron uptake by *A. baumannii*

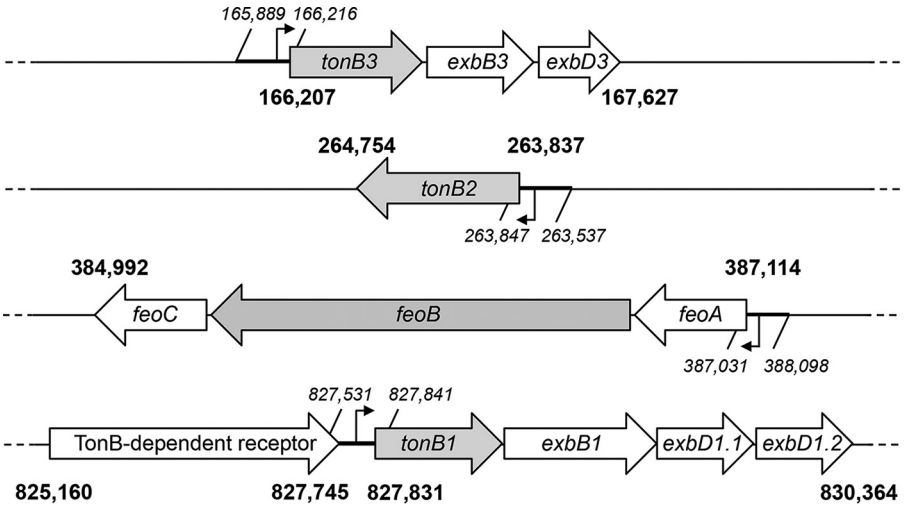

FIG 1 Genetic organization of the *A. baumannii* ATCC 19606^T TonB and Feo systems. The ca. 3.9-Mb genome of *A. baumannii* ATCC 19606^T contains a *feoABC* operon and three *tonB* gene clusters. The *tonB1* and *tonB3* genes are part of typical *tonB-exbB-exbD* operons, while *tonB2* is a monocistronic element. Nucleotide positioning of these gene loci on the *A. baumannii* ATCC 19606^T genome is indicated in bold. The three *tonB* genes and the *feoA* gene are preceded by putative promoter elements, whose nucleotide positioning on the *A. baumannii* ATCC 19606^T genome is indicated in italic.

ATCC 19606^T, individual markerless *tonB1*, *tonB2*, *tonB3*, or *feoB* deletion mutants were generated as described in Materials and Methods (22). Multiple mutants lacking Feo and/or TonB were also obtained (Table 1). The wild type and isogenic iron uptake mutants were tested for their ability to grow under different conditions of iron availability, i.e., in M9 minimal medium and in M9 supplemented with either the iron chelator 2,2′-dipyridyl (DIP) or ferric chloride ($FeCl_3$) (Fig. 2). The growth of the Δ*tonB1* and Δ*tonB2* mutants did not differ from that of the parent strain, regardless of the test condition (Fig. 2). The isogenic Δ*feoB* mutant also showed growth profiles similar to those of the wild type (Fig. 2), suggesting that ferrous iron acquisition is not essential for *A. baumannii* growth under these conditions. In contrast, the growth of the Δ*tonB3* mutant was completely abrogated in both M9 (Fig. 2A) and M9 supplemented with 100 μM DIP (Fig. 2B). All multiple mutants carrying the *tonB3* mutation (i.e., the Δ*tonB3* Δ*feoB*, Δ*tonB1* Δ*tonB2* Δ*tonB3* and Δ*tonB1* Δ*tonB2* Δ*tonB3* Δ*feoB* mutants) were unable to grow under iron-limiting conditions (see Fig. S1A and B in the supplemental material). Growth of the *tonB3* mutants was rescued by constitutive (P*tac*-dependent) expression of *tonB3* via the pME6031-derived plasmid pME*tonB3* (Fig. 2A and B) and by the exogenous provision of 100 μM $FeCl_3$ (Fig. 2C and S1C), even though growth of the *tonB3* mutant in the presence of 100 μM $FeCl_3$ was delayed compared with that of the wild type (Fig. 2C and S1C). The empty vector pME6031, used as a control, did not affect the growth profile of *A. baumannii* ATCC 19606^T (data not shown). These results demonstrate that the ability of *A. baumannii* to grow in iron-poor media strictly depends on the TonB3 system, as opposed to the TonB1 and TonB2 systems, which appear to be dispensable under the test conditions.

Increased siderophore production is a hallmark of intracellular iron deficiency (23), and hence, the ability of the Δ*tonB* and Δ*feo* mutants to produce siderophores was assessed using the chrome azurol S (CAS) agar assay (24). We observed increased siderophore production for the single and multiple Δ*tonB3* mutants compared with the parental strain, resulting in larger orange halos around the bacterial colonies (Fig. 3A; see Fig. S2A in the supplemental material). In the Δ*tonB3* mutant, this phenotype was rescued by complementation with pME*tonB3* (Fig. 3A). Conversely, the *tonB1*, *tonB2*, and *feoB* mutations had no effect on the production of siderophores (Fig. 3A).

To directly correlate growth capabilities and siderophore production with intracellular iron levels, the total iron contents in ATCC 19606^T and the Δ*tonB1*, Δ*tonB2*, Δ*tonB3*,

TABLE 1 Bacterial strains and plasmids used in this study

Strain or plasmid	Relevant characteristics[a]	Reference or source
Strains		
A. baumannii		
ATCC 19606^T	Clinical isolate; type strain	ATCC
Δ*feoB* mutant	ATCC 19606^T containing a 1,681-bp deletion in the *feoB* gene	This study
Δ*tonB1* mutant	ATCC 19606^T containing a 693-bp deletion in the *tonB1* gene	This study
Δ*tonB2* mutant	ATCC 19606^T containing a 585-bp deletion in the *tonB2* gene	This study
Δ*tonB3* mutant	ATCC 19606^T containing a 852-bp deletion in the *tonB3* gene	This study
Δ*tonB3* Δ*feoB* mutant	Δ*tonB3* mutant containing a 1,681-bp deletion in the *feoB* gene	This study
Δ*tonB1* Δ*tonB2* Δ*tonB3* mutant	ATCC 19606^T with deletions in all three *tonB* genes	This study
Δ*tonB1* Δ*tonB* Δ*tonB3* Δ*feoB* mutant	ATCC 19606^T with deletions in all three *tonB* genes and containing a 1,681-bp deletion in the *feoB* gene	This study
ATCC 19606^T(pME6031)	ATCC 19606^T harboring pME6031, empty vector	This study
Δ*tonB3*(pME*tonB3*) mutant	Δ*tonB3* harboring pME6031, containing the *tonB3* gene	This study
Δ*feoB*(pME*feoAB*) mutant	Δ*feoB* harboring pME6031, containing the *feoAB* genes	This study
E. coli		
DH5α	*recA1 endA1 hsdR17 supE44 thi-1 gyrA96 relA1* Δ(*lacZYA-argF*)*U169* (ϕ80d*lacZ*ΔM15) F$^-$ Nal^r	59
H1717	*fhuF::λplacMu aroB araD139* Δ*lacU169 rpsL150 relA1 flbB5301 deoC1 ptsF25 rbsR*	27
Plasmids		
pBIISK_*sacB/kanR*	Suicide vector for allelic replacement; Km^r	22
pME6031	Expression vector for genetic complementation; P*tac* Δ*lacI*^{q}; Tc^r	60
pBluescript-II KS	Standard cloning vector; ColE1 replicon; Ap^r	Stratagene
pMP220	Broad-host-range, low-copy-number promoter-probe vector; Tc^r	67
pME*tonB3*	pME6031 containing the *tonB*3 gene (promoter and coding region); Tc^r	This study
pME*feoAB*	pME6031 containing the *feoAB* genes (promoter and coding region); Tc^r	This study
pBSP_{tonB1}	pBS containing the *tonB1* putative promoter region; Ap^r	This study
pBSP_{tonB2}	pBS containing the *tonB2* putative promoter region; Ap^r	This study
pBSP_{tonB3}	pBS containing the *tonB3* putative promoter region; Ap^r	This study
pBSP_{feoA}	pBS containing the *feoA* putative promoter region; Ap^r	This study
pBSP_{basA}	pBS containing the *basA* promoter region; Ap^r	26
pMPP_{tonB1}	pMP220 containing the *tonB1* putative promoter region; Tc^r	This study
pMPP_{tonB2}	pMP220 containing the *tonB2* putative promoter region; Tc^r	This study
pMPP_{tonB3}	pMP220 containing the *tonB3* putative promoter region; Tc^r	This study
pMPP_{feoA}	pMP220 containing the *feo* putative promoter region; Tc^r	This study
pMPP_{basA}	pMP220 containing the *basA* promoter region; Tc^r	26

[a]Nal^r, nalidixic acid resistance; Km^r, kanamycin resistance; Tc^r, tetracycline resistance; Ap^r, ampicillin resistance.

and Δ*feoB* mutants was compared by means of inductively coupled plasma optical emission spectrometry (ICP-OES). Due to growth impairment of the *tonB3* mutant under low-iron conditions, bacteria were precultured in M9 supplemented with 20 μM $FeCl_3$, washed twice with saline, diluted in M9 supplemented with 1 μM $FeCl_3$ (the minimum concentration supporting some growth of the *tonB3* mutant), and then incubated at 37°C with shaking for 60 h (to obtain sufficient biomass of the *tonB3* mutant for ICP-OES measurements of intracellular iron). In line with the prominent role of TonB3 in iron uptake and despite 1 μM $FeCl_3$ supplementation, the intracellular iron content was strongly reduced (more than 2-fold) in the Δ*tonB3* mutant compared with the parent strain, and this phenotype was partially complemented by the pME*tonB3* plasmid (Fig. 3B). Conversely, the intracellular iron contents were comparable in the Δ*tonB1*, Δ*tonB2*, Δ*feoB*, and parent strains (Fig. 3B).

Overall, these data demonstrate that TonB3-deficient *A. baumannii* is unable to grow in an iron-poor medium as a consequence of its inability to acquire iron from the environment, supporting a pivotal role of TonB3 in Fe(III) acquisition.

Iron controls the expression of the *tonB3* and *feo* genes through the global regulator Fur. Iron uptake systems are usually expressed under iron-limiting conditions. To investigate the expression of the *tonB* and *feoB* genes in response to iron concentration, the putative promoter regions of the *tonB1* (P_{tonB1}), *tonB3* (P_{tonB3}), and *feo* (P_{feoA}) operons and of the *tonB2* gene (P_{tonB2}) (Fig. 1) were identified by *in silico* predictions using the BPROM tool of the SoftBerry suite for bacterial promoters (25),

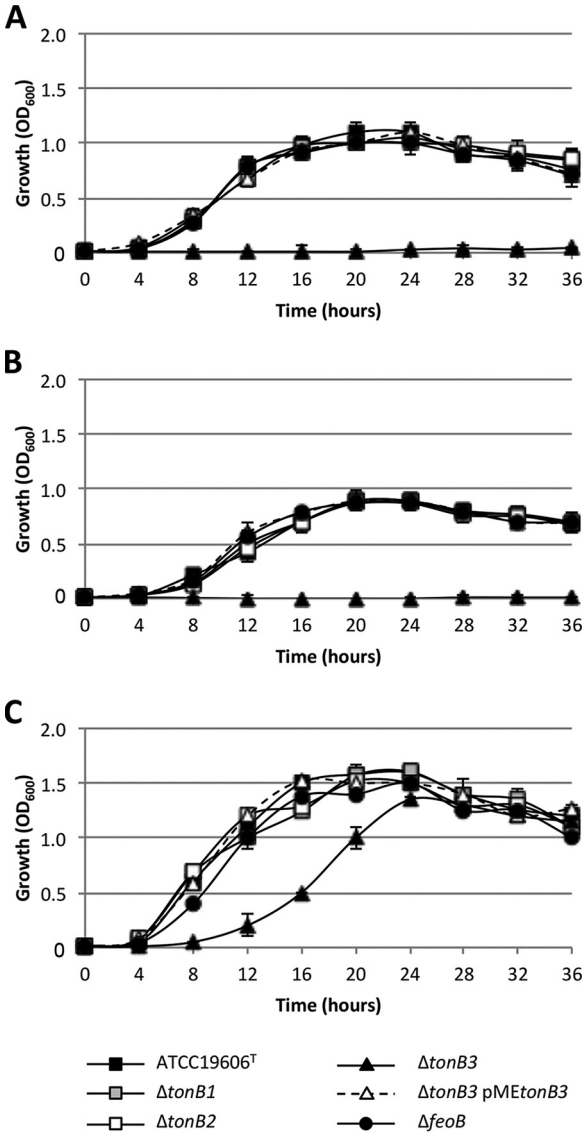

FIG 2 Effect of *tonB* and *feo* deletion on *A. baumannii* growth. Growth curves of *A. baumannii* ATCC 19606^T and *tonB* and *feo* mutants in M9 minimal medium (A), M9 supplemented with 100 μM DIP (B), and M9 supplemented with 100 μM $FeCl_3$ (C) are shown. Values are the means from three independent experiments ± standard deviation.

and large DNA fragments (310 to 1,067 nucleotides [nt]) encompassing the predicted promoter regions were cloned in the promoter-probe vector pMP220. Promoter activity was measured as β-galactosidase levels expressed by *A. baumannii* ATCC 19606^T carrying individual promoter fusions under iron-depleted (i.e., M9 plus 100 μM DIP) or iron-replete (i.e., M9 plus 100 μM $FeCl_3$) conditions (Fig. 4A). As a control, the pMP220 derivative plasmid containing the promoter region of the iron-regulated gene *basA* was used (26). Similar to the case for P_{basA}, the activity of both the P_{tonB3} and P_{feoA} predicted promoters was increased by ca. 3-fold under iron-depleted relative to iron-replete conditions. Conversely, no iron regulation was observed for the predicted P_{tonB1} and P_{tonB2}. Of note, β-galactosidase activity for the P_{tonB1} putative promoter was barely detectable (<60 Miller units), suggesting that the *tonB1* operon is poorly expressed, at least under the test conditions.

To corroborate these data, real-time PCR analyses were performed on total RNA extracted from *A. baumannii* ATCC 19606^T grown in M9 and in M9 supplemented with either 100 μM DIP or 100 μM $FeCl_3$ (Fig. 4B). The mRNA levels of the *tonB3*, *feoB*, and

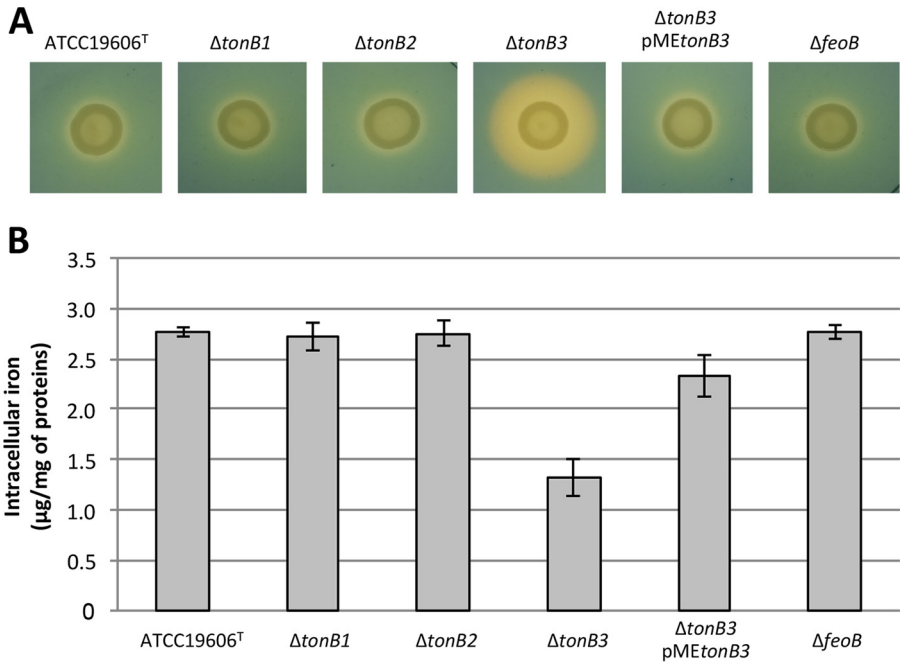

FIG 3 Production of iron-chelating compounds and intracellular iron content of *A. baumannii* iron uptake mutants. (A) Production of iron-chelating compounds (siderophores) on CAS agar plates, as detectable by the formation of an orange halo surrounding the colonies of the indicated bacterial strains. Images are representative of three independent experiments giving similar results. (B) Amount of intracellular iron (normalized to the total protein content) in the indicated strains grown in M9 supplemented with 1 μM $FeCl_3$, determined by ICP-OES analysis (see Materials and Methods for experimental details). Values are the means from three independent experiments ± the standard deviation.

basA genes were significantly increased under iron-limited conditions (i.e., in M9 and M9 plus 100 μM DIP relative to M9 plus 100 μM $FeCl_3$), thus confirming that the expression of *tonB3* and *feo* genes is upregulated by iron starvation. Conversely, no significant difference was observed for *tonB1* and *tonB2* expression (Fig. 4B), in accordance with literature data (6). Raw data from the real-time PCR analyses confirmed low levels of *tonB1* mRNA (high absolute threshold cycle [C_T] values at the threshold [data not shown]), consistent with low activity of the P_{tonB1} promoter (Fig. 4A).

Iron homeostasis in Gram-negative bacteria is controlled primarily by the global transcriptional repressor Fur (9). Our *in silico* analysis revealed the presence of a putative Fur box in both P_{tonB3} (encompassing the predicted −10/−35 sequences) and P_{feoA} (downstream of the predicted transcriptional start site) (Fig. 4C). Conversely, no Fur boxes could be identified in the P_{tonB1} and P_{tonB2} putative promoter regions. *In vivo* binding of Fur to P_{tonB3} and P_{feoA} was investigated by the Fur titration assay (FURTA) (27). To this end, pBluescript (pBS)-derived plasmids containing the P_{tonB1}, P_{tonB2}, P_{tonB3}, and P_{feoA} promoter regions were generated. As controls, the empty vector pBS and a pBS-derived plasmid containing the Fur-controlled P_{basA} promoter were used. As expected, *E. coli* H1717 cells harboring pBSP_{basA} formed red colonies (Lac^+) on MacConkey agar supplemented with 100 μM $FeSO_4$, in accordance with literature data (26), and the same phenotype was observed in the H1717 strains carrying pBSP_{tonB3} or pBSP_{feoA} (Fig. 4D). Conversely, *E. coli* H1717 containing pBS, pBSP_{tonB1}, or pBSP_{tonB2} generated white (Lac^-) colonies in the same medium (Fig. 4D). Similar results were obtained for MacConkey agar plates supplemented with lower $FeSO_4$ concentrations (i.e., 25 and 50 μM; see Fig. S3 in the supplemental material). Indeed, the pBS, pBSP_{tonB1}, and pBSP_{tonB2} constructs turned white at 25 μM $FeSO_4$, while pBSP_{tonB3} and pBSP_{feoA} remained red up to 100 μM $FeSO_4$ (Fig. 4D and S3). Therefore, both the *tonB3* and *feo* genes are repressed by the transcriptional regulator Fur when the intracellular iron content is high enough to enable Fur binding to the predicted Fur boxes located within the P_{tonB3} and P_{feoA} promoters.

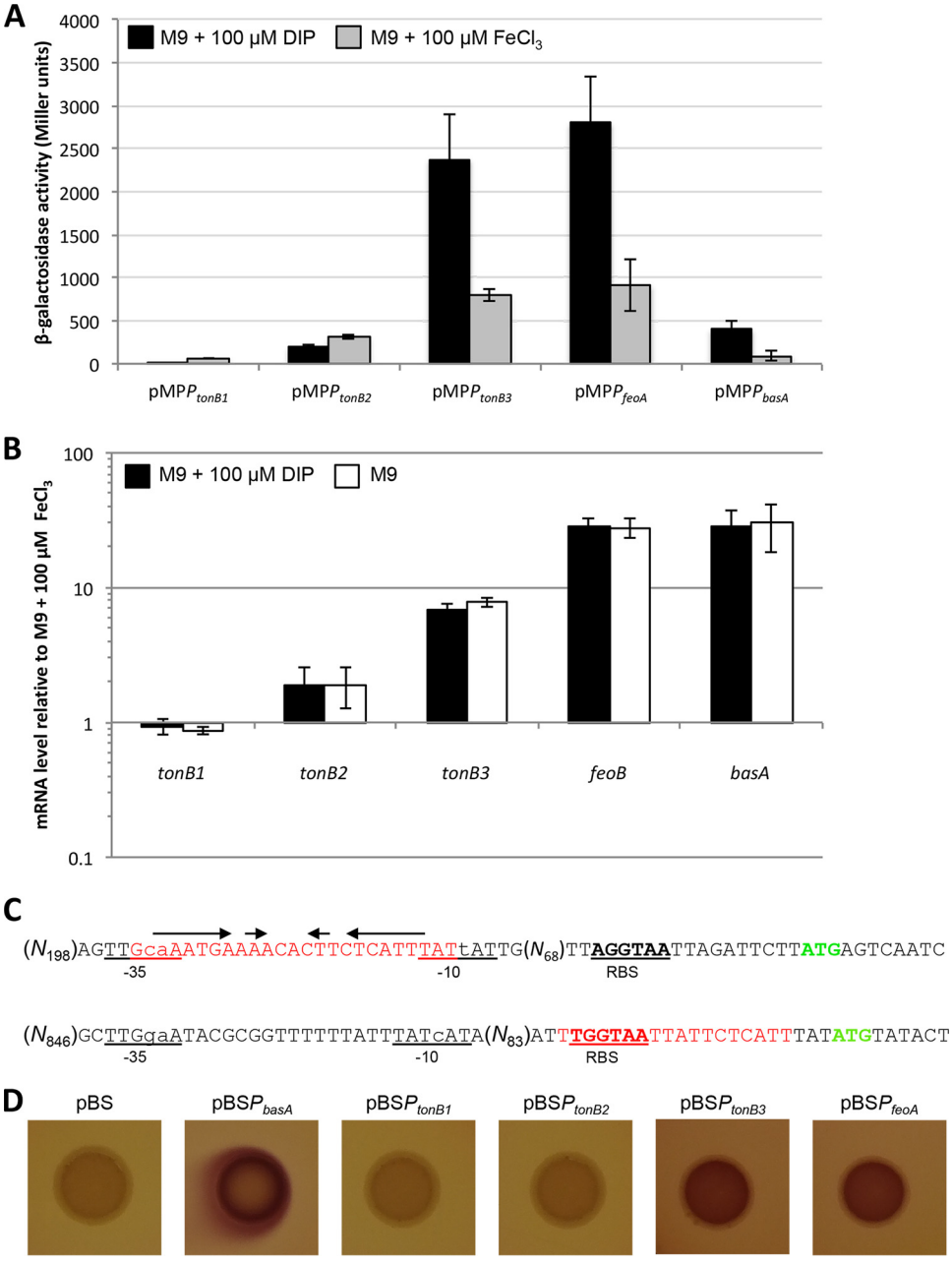

FIG 4 Expression analysis of *tonB* and *feo* genes in *A. baumannii* ATCC 19606^T. (A) β-Galactosidase activity measured in *A. baumannii* ATCC 19606^T strains carrying the indicated plasmids, grown in M9 supplemented with 100 μM DIP (black bars) or with 100 μM $FeCl_3$ (gray bars). Mean values from three independent experiments ± standard deviation are shown. (B) Relative mRNA levels of the indicated genes, quantified by real-time PCR in *A. baumannii* ATCC 19606^T grown in M9 (white bars) or in M9 supplemented with 100 μM DIP (black bars), relative to those in the same strain grown in M9 supplemented with 100 μM $FeCl_3$. Mean values from three independent experiments ± standard deviation are shown. (C) The P_{tonB3} (upper sequence) and P_{feoA} (lower sequence) putative promoter regions, with the predicted −35 and −10 sequences (underlined), the predicted ribosome-binding site (RBS) (underlined and in bold), the ATG start codon (green and in bold), and the predicted Fur box (red) shown; inverted repeats are indicated with arrows. Prediction of the −10 and −35 hexamers was based on RpoD-dependent *E. coli* promoters (consensus, TTGACA-N17 ± 1-TATAAT) (66). The *tonB3* predicted promoter sequence is TTGcaA-N18-TATtAT, while the *feoA* predicted promoter sequence is TTGgaA-N16-TATcAT (lowercase denotes differences from the *E. coli* consensus). (D) FURTA. *E. coli* H1717 strains carrying the indicated plasmids were grown for 24 h on MacConkey agar supplemented with 100 μM $FeSO_4$. Images are representative of three independent experiments giving similar results (also see Fig. S3 in the supplemental material).

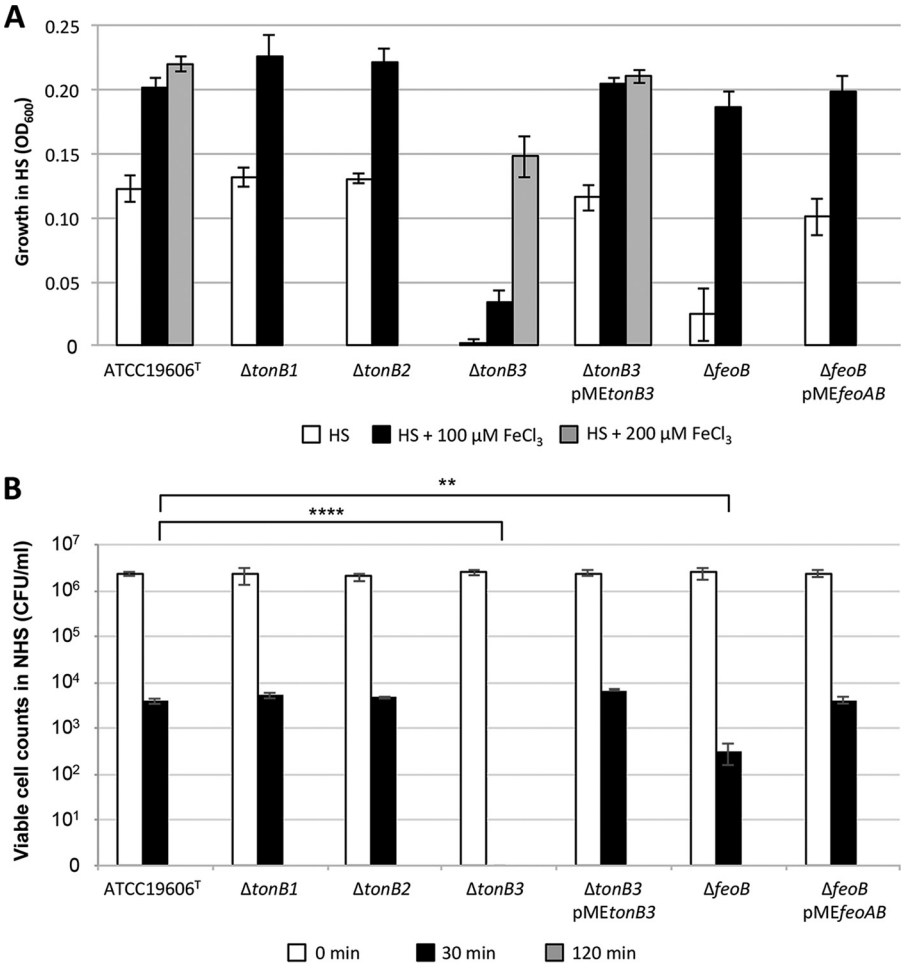

FIG 5 Growth of *A. baumannii* iron uptake mutants in HS and their susceptibility to NHS. (A) The indicated bacterial strains were cultured in HS in the absence of $FeCl_3$ (white bars) or in the presence of 100 μM $FeCl_3$ (black bars) or 200 μM $FeCl_3$ (gray bars). Cell density (OD_{600}) was determined after 48 h of incubation at 37°C with shaking. Values are the means from three independent experiments ± the standard deviation. (B) Suspensions of the indicated bacterial strains were exposed to NHS at 37°C for 0 min (white bars), 30 min (black bars), or 120 min (gray bars) before determination of viable cell counts on LB agar plates. Data are the means from three independent experiments (± the standard deviation). Asterisks denote statistically significant differences, measured 30 min after NHS challenge, between ATCC 19606^T and the Δ*tonB3* (****, $P < 0.0001$) or Δ*feoB* (**, $P < 0.01$) mutant. Differences between ATCC 19606^T and the other strains are not statistically significant at 30 min. For all strains, no viable cell was detected after 120 min of incubation in NHS.

The *tonB3* and *feo* mutations reduce *A. baumannii* growth in complement-free HS and increase susceptibility to the bactericidal activity of NHS. To unravel the importance of iron uptake during *A. baumannii* infection, *A. baumannii* ATCC 19606^T and isogenic iron uptake-defective mutants were cultured in heat-inactivated human serum (HS), in which transferrin is expected to exert a bacteriostatic effect due to iron sequestration. HS somehow mimics the medium encountered by bacteria disseminating in biological fluids during a systemic infection. Since *A. baumannii* grows slowly in HS (26, 28), the bacterial cell density was determined at 48 h postinoculation (Fig. 5A). As expected, the Δ*tonB3* strain was unable to grow in HS. Supplementation of HS with 100 μM $FeCl_3$ was not sufficient to chemically complement the *tonB3* mutation, likely due to Fe(III) binding by serum transferrin. However, the cell density of the Δ*tonB3* strain was restored to wild-type levels by exogenous provision of a higher $FeCl_3$ concentration (200 μM) or by plasmid-driven expression of a functional *tonB3* gene (the Δ*tonB3* pME*tonB3* strain). Likewise, no growth in HS was observed for the Δ*tonB3*

multiple mutants (i.e., the Δ*tonB1* Δ*tonB2* Δ*tonB3* and Δ*tonB1* Δ*tonB2* Δ*tonB3* Δ*feoB* mutants) (see Fig. S4 in the supplemental material).

Growth of the Δ*tonB1* and Δ*tonB2* mutants in HS and in HS supplemented with 100 μM $FeCl_3$ was comparable to that of the parental strain (Fig. 5A), strengthening the evidence that these two systems are not primarily implicated in *A. baumannii* iron uptake.

In contrast to what was observed in M9 (Fig. 2), *feoB* deletion caused a 4-fold decrease of *A. baumannii* cell density in HS compared to that of the parental strain, and this growth defect could be complemented to wild-type levels both chemically (i.e., by addition of 100 μM $FeCl_3$ to HS) and genetically (i.e., by in *trans* expression of *feoB* from the pME*feoAB* plasmid) (Fig. 5A).

These results underscore the importance of TonB3 for iron uptake also in biological fluids and indicate that the Feo system contributes to bacterial proliferation in HS.

Besides iron uptake, features that facilitate the persistence of *A. baumannii* in the host include the capacities to adhere to biotic and abiotic surfaces, to form biofilm, and to resist to the complement-mediated killing of normal human serum (NHS) (29). Thus, we evaluated these virulence-related traits in TonB and Feo mutants. Briefly, biofilm formation and membrane properties linked to surface adherence (i.e., outer membrane stability and hydrophobicity) were comparable for *A. baumannii* ATCC 19606^T and all tested mutants (see Fig. S5 in the supplemental material). Conversely, the Δ*tonB3* mutant and, to a lesser extent, the Δ*feoB* mutant displayed increased susceptibility to the (complement-dependent) bactericidal activity of NHS compared with that of the parent strain and the Δ*tonB1* and Δ*tonB2* mutants (Fig. 5B). In fact, exposure to 90% NHS for 30 min caused a ca. 3-log reduction in the viability of wild-type *A. baumannii* ATCC 19606^T and the Δ*tonB1* and Δ*tonB2* mutants relative to that of preexposed cultures (0 min), while viability of the Δ*feoB* mutant was reduced by ca. 4 logs and all the cells of the Δ*tonB3* mutant were killed by NHS in 30 min (Fig. 5B). Reversal to wild-type-level susceptibility to NHS was observed for both the Δ*feoB* and Δ*tonB3* mutants upon complementation with the pME*feoAB* and pME*tonB3* plasmids, respectively (Fig. 5B). Notably, all the tested strains were killed by NHS exposure for 120 min (Fig. 5B).

As a whole, the above findings denote a primary implication of *tonB3* in *A. baumannii* Fe(III) uptake and resistance to complement-dependent killing in human serum.

TonB3 is essential for *A. baumannii* virulence in insect and mammalian infection models. It has previously been observed that siderophore systems are involved in *A. baumannii* virulence (4, 6, 30). Here, the role of iron uptake mutants in *A. baumannii* virulence was initially screened by using the *Galleria mellonella* infection model, since it was previously used to investigate the virulence of the Δ*tonB1* and Δ*tonB2* mutant strains (6). Larvae were infected with ca. 1×10^6 CFU of the parental strain *A. baumannii* ATCC 19606^T or the derivative iron uptake mutants, and viability was monitored daily for 72 h (Fig. 6A; see Fig. S6 in the supplemental material).

About 60% of caterpillars infected with the parental strain ATCC 19606^T were killed 3 days after injection (Fig. 6A). Interestingly, the *tonB3* deletion mutant killed only 10% of the injected larvae after 72 h ($P < 0.0001$), while deletion of *tonB1* and *tonB2* had no effect on *A. baumannii* ATCC 19606^T lethality (Fig. 6A). The killing ability of the Δ*feoB* mutant was slightly reduced (50% of larvae killed 72 h postinjection) (Fig. 6A) compared with that of the parental strain, but this difference was not statistically significant ($P = 0.2256$). Only minor, nonsignificant differences were observed in the percentages of larvae killed by the Δ*tonB3* single mutant or by multiple mutants with *tonB3* deletion (Fig. S6). These results demonstrate that the TonB3 system is strictly required for *A. baumannii* lethality in *G. mellonella*, as opposed to the TonB1, TonB2, and Feo systems.

To corroborate the key role of TonB3 in *A. baumannii* ATCC 19606^T pathogenicity, the virulence of the parental strain and of iron uptake mutants was compared in a mouse model of intraperitoneal (i.p.) infection (31). Preliminary screenings were performed on a small number of mice (1 to 3 per strain) to select for iron uptake systems relevant to *A. baumannii* virulence in this infection model. It was noticed that only the

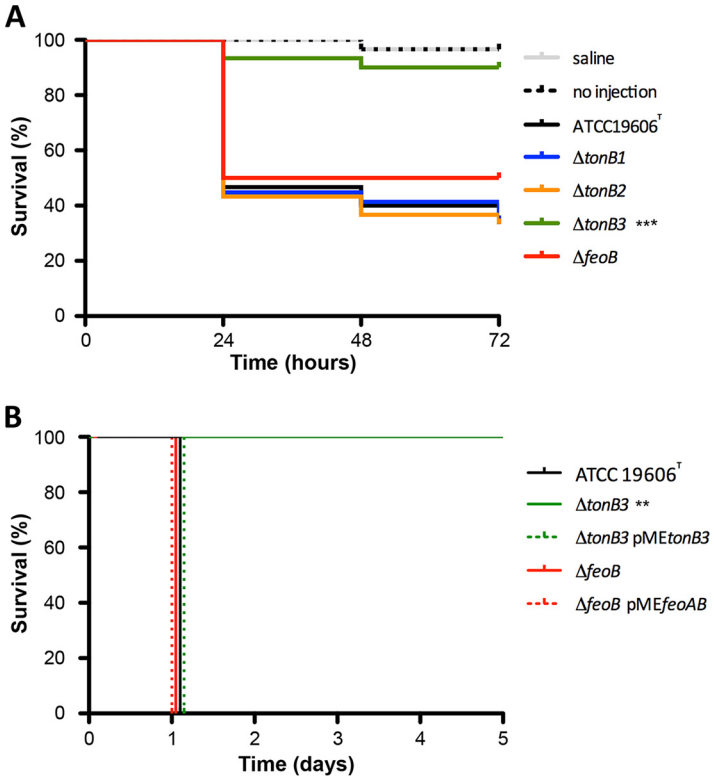

FIG 6 Impact of the TonB and Feo systems on *A. baumannii* virulence in animal models. (A) *G. mellonella* larvae ($n = 30$) were injected with ca. 1×10^6 CFU of the indicated strains. As a control, larvae were injected with saline or not injected. Larvae were incubated at 37°C and monitored daily for 72 h. ***, $P < 0.0001$ (log rank test). (B) Groups of five BALB/c mice were inoculated i.p. with ca. 10^5 CFU of the indicated strains. Their clinical signs and survival were monitored daily for 5 days. The inocula were 0.9×10^5 CFU for ATCC 19606^T, 0.6×10^5 CFU for the Δ*feoB* mutant, 0.4×10^5 CFU for the Δ*feoB*(pME*feoAB*) mutant, 0.8×10^5 CFU for the Δ*tonB3* mutant, and 0.5×10^5 CFU for the Δ*tonB3*(pME*tonB3*) mutant. **, $P < 0.001$ (log rank test).

mice infected with *A. baumannii* mutants with deletions in the *tonB3* gene survived the challenge (see Table S1 in the supplemental material). Although the Δ*feoB* strain killed the infected mice in the preliminary experiment, this mutant was further investigated due to its growth defect in HS. Therefore, in a subsequent experiment, groups of 5 mice were inoculated i.p. with ca. 10^5 CFU of *A. baumannii* ATCC 19606^T or of the Δ*tonB3* or Δ*feoB* mutant carrying or not carrying the complementing pME*tonB3* or pME*feoAB* plasmid, respectively. Survival of the infected mice was monitored every 24 h for 5 days. As shown in Fig. 6B, the *tonB3* mutation completely abrogated *A. baumannii* virulence in mice (100% survival), and genetic complementation with pME*tonB3* fully restored lethality. Conversely, all the mice infected with the Δ*feoB* or Δ*feoB*(pME*feoAB*) strain died within 24 h after the challenge, like the mice infected with the wild-type strain (Fig. 6B). These *in vivo* data provide conclusive evidence that TonB3 is essential for *A. baumannii* ATCC 19606^T virulence in different animal models, whereas the TonB1, TonB2, and Feo systems appear to be dispensable.

DISCUSSION

Colonization and infection are strictly dependent on the ability of pathogenic bacteria to acquire iron from their host (7). In turn, mammals respond to the infection by nutritional immunity, i.e., increasing iron sequestration and storage to withhold this essential metal from invading pathogens (32). As a consequence, bacterial pathogens have evolved numerous mechanisms to scavenge iron from host proteins during the infection.

Ferrous iron uptake appears to be more important than ferric iron transport for a

number of bacteria, including enteropathogenic *E. coli* (33), *Helicobacter pylori* (34), and *Clostridium perfringens* (35), suggesting that in low-oxygen or low-pH environments (e.g., the intestine or gastric mucosa), Fe(II) uptake could be the preferred pathway for bacterial iron acquisition. This is not the case for the aerobic species *A. baumannii*, which is found predominantly in oxygen-rich environments. In contrast to Fe(III), Fe(II) is thought to passively diffuse across the porins on the Gram-negative outer membrane (11), thus not requiring a TonB-energy transduction component to reach the periplasm. However, at neutral pH and in the presence of oxygen, Fe(II) is rapidly oxidized to Fe(III), which is likely to be the main iron form encountered by *A. baumannii* in aerobic environments, suggesting a predominant role of Fe(III) over Fe(II) acquisition in this pathogen. Accordingly, our results demonstrate that *feoB* deletion does not impair *A. baumannii* growth in an iron-poor medium (Fig. 2A), even after supplementation with the iron-chelating agent DIP (Fig. 2B). We also observed that knocking out the Feo system neither affects siderophore production (Fig. 3A) nor reduces *A. baumannii* virulence (Fig. 6). Of note, all *in vitro* assays described in this study were performed under aerobic conditions in the absence of reducing agents; thus, only a minimal amount of ferrous iron would be available for transport by the Feo system in our experimental settings. Intriguingly, we found that the Feo system was required for full growth of *A. baumannii* in HS and for resistance to the bactericidal activity of NHS, as also suggested by previous work (36) (Fig. 5). These phenotypes could be attributed to host-derived antimicrobial peptides, since the *feoB* mutant was previously shown to be hypersensitive to human serum complement and to polymyxin B (which somehow mimics the activity of antimicrobial peptides) compared to the parental strain (36). Considering the significant mortality (34%) associated with *A. baumannii* bloodstream infection in nosocomial settings (ranking third after *Candida* spp. and *P. aeruginosa*) (37), the possible role of the Feo system in ferrous iron acquisition during systemic infection cannot be excluded.

Assays in M9 minimal medium revealed that deletion of either *tonB1* or *tonB2* does not affect *A. baumannii* growth under iron-limiting conditions, as opposed to the deletion of *tonB3*, which completely abrogated growth (Fig. 2; see Fig. S1 in the supplemental material). These data demonstrate the essential role of TonB3 in sustaining *A. baumannii* growth under conditions of iron starvation, arguing for a functional predominance of the TonB3-dependent over the TonB1- and TonB2-dependent iron uptake system. The key role of TonB3 in Fe(III) uptake is also corroborated by retarded growth of the *tonB3*-deficient strains even in the presence of 100 μM $FeCl_3$ (Fig. 2C and S1), although still-unknown functions of TonB3, unrelated to iron uptake, could contribute to this phenotype. Altogether, these findings add novel insights to previously published work, not only confirming the minor role played by the individual TonB1 and TonB2 systems in iron uptake by *A. baumannii* (6) but also providing an experimental proof of the formerly envisaged prominent role of TonB3 (6).

Besides *A. baumannii*, many Gram-negative bacteria harbor multiple genes coding for TonB proteins (6, 38–40). TonB proteins are known for providing energy to different high-affinity transport systems, which allow bacteria to acquire several nutrients, such as vitamin B_{12} (41), ferric siderophores (42), and hemin and heme (43). A number of TonB-dependent transporters have previously been identified in *A. baumannii* genomes (8), suggesting that the TonB complex could serve as a polyvalent energy coupler for functioning of multiple TonB-dependent transporters and that multiple TonB orthologs may accomplish different functions. Although TonB1 and TonB2 seem to be dispensable for growth under the experimental conditions used in this work, they could be involved in other TonB-dependent membrane-associated processes. Indeed, TonB2 seems to be involved in *A. baumannii* adhesion to human alveolar epithelial cells (6). Similar results were previously described for the opportunistic human pathogen *P. aeruginosa*, which carries three *tonB* homologs. It has been shown that in *P. aeruginosa*, only *tonB1* (the gene orthologous to *A. baumannii tonB3*) is required for growth under iron limitation (17), while *tonB3* is involved mainly in motility and pilus assembly (44).

While outer membrane transporters functionally associated with individual *A. bau-*

mannii TonB proteins are not well defined at present, it can be speculated that TonB3 can serve as an energy coupler for more than one transporter, given that 20 putative TonB-dependent transporters have been identified in the annotated *A. baumannii* ATCC 19606^T genome (https://www.ncbi.nlm.nih.gov/genome/proteins/403?genome_assembly_id=165902), many of them being genetically associated with siderophore and heme receptors (8). A plausible candidate for TonB3-dependent transport is the acinetobactin siderophore receptor BauA (45, 46), since an *entA* mutant impaired in acinetobactin biosynthesis did not grown in iron-poor media (6), thus showing a phenotype similar to that of the *tonB3* mutant. Since deletion mutants for the three *A. baumannii* ATCC 19606^T *tonB* paralogs are available, functional associations between individual TonB-dependent transporters and TonB systems have now become feasible.

Experimental evidence obtained from FURTA and mRNA quantification indicates that both *tonB3* and *feo* are iron regulated, consistent with the identification in their promoter sequences of putative Fur boxes showing similarity with the *A. baumannii* Fur consensus (Fig. 4) (47). Being impaired in iron uptake, the *tonB3* mutant contains lower intracellular iron levels and overproduces siderophores (Fig. 3) as a compensatory response to iron scarcity and dysregulated Fur function.

No substantial difference in outer membrane stability, hydrophobicity, or biofilm formation was observed between iron uptake mutants (see Fig. S4 in the supplemental material). However, it should be taken into account that in these experimental settings the Δ*tonB3* mutant required supplementation of iron to the medium, albeit at a low concentration, to achieve sufficient growth. Notably, both the *feoB* and *tonB3* mutants showed faster and more significant killing by NHS than the wild type and other *tonB* mutants. Indeed, the *tonB3* deletion increased *A. baumannii* susceptibility to NHS more severely than *feoB* deletion (Fig. 5B), further supporting the key role played by the TonB3 system in host colonization. Future experiments are required to clarify the molecular mechanisms underlying increased susceptibility of the Δ*tonB3* mutant to NHS.

In some bacterial species, *tonB* mutants exhibit a dramatic attenuation of virulence compared to the parental strains (21, 48–51). In this study, animal experiments revealed that mutants with deletions in the *tonB3* gene are less virulent than the wild type, whereas *tonB1* and *tonB2* mutations do not affect *A. baumannii* virulence (Fig. 6). The negligible effect of single *tonB1* or *tonB2* mutation on killing of *G. mellonella* larvae by *A. baumannii* is in agreement with literature data (6) and emphasizes the prominent role of TonB3, and hence of iron uptake, in this animal model of infection. *G. mellonella* is considered a suitable organism for bacterial pathogenicity screening, since this insect model of infection bypass the logistical, ethical, and financial barriers of mammalian models. However, the use of mammals for evaluating the virulence of microbial pathogens provides more complete information on the host-pathogen interactions. In our case, a good correlation exists between virulence in *G. mellonella* larvae and in mice, corroborating the utility of *G. mellonella* as a "screening tool" to select a limited number of strains to be subsequently tested in mice.

Many studies have exploited the possibility of developing antibacterial strategies targeting siderophores biosynthesis (52, 53). However, in many pathogens, including *A. baumannii*, the use of inhibitors of specific siderophore biosynthetic enzymes could be problematic due to the multiplicity of iron acquisition systems (8). This functional redundancy complicates the identification and development of drugs that successfully inhibit bacterial growth by targeting iron uptake. Common players in the iron acquisition machinery, rather than individual iron acquisition systems, are more promising targets for broad-range therapeutic approaches. Indeed, antibacterial compounds targeting iron acquisition (i.e., TonB) have already been explored in uropathogenic *E. coli* (54), and molecules targeting TonB systems gave encouraging results when tested on *A. baumannii* (55). As to TonB3 druggability, it is important to underline that *tonB3* is among the genes whose expression is upregulated during bacteremia (56) and that no homologs of TonB3 have so far been identified in mammals, hopefully limiting toxicity

issues related to the administration of TonB3 inhibitors. Moreover, some studies indicate that avirulent *tonB* mutants represent suitable backbone strains for future vaccine development against *Klebsiella pneumoniae*, *Burkholderia mallei*, and *Burkholderia cenocepacia* infections (51, 57, 58). Given the increasing antibiotic resistances of *A. baumannii* and the essentiality of iron for *A. baumannii* growth *in vivo*, the data presented in this study highlight TonB3 as a suitable target for the development of new antimicrobial compounds and pave the way to testing *tonB3* mutants as attenuated *A. baumannii* vaccines.

MATERIALS AND METHODS

Bacterial strains and culture conditions. The strains and plasmids used in this study are listed in Table 1. *A. baumannii* ATCC 19606^T, *E. coli* DH5α, and *E. coli* H1717 were grown at 37°C in Luria-Bertani broth (LB) and LB agar (LA) or in M9 minimal medium containing 20 mM sodium succinate as the carbon source (59). Ampicillin (Ap), kanamycin (Km), and tetracycline (Tc) were added when required at the following concentration: for *E. coli*, 100 μg/ml Ap, 20 μg/ml Km, and 12.5 μg/ml Tc; for *A. baumannii*, 50 μg/ml Km and 50 μg/ml Tc.

Markerless mutagenesis and genetic complementation. Markerless *A. baumannii* iron uptake mutants were generated as previously described (22). Briefly, upstream and downstream DNA regions of *feoB*, *tonB1*, *tonB2*, and *tonB3* (ca. 1,500 bp each) were cloned in the suicide vector pBIISK_*sacB/kanR*. The resulting plasmids were used for allelic exchange in *A. baumannii* ATCC 19606^T (22). Km-sensitive colonies were verified by PCR using appropriate primer pairs (see Table S2 in the supplemental material). For the *tonB3* mutant, growth media were supplemented with 50 μM $FeSO_4$. Mutants were complemented with the pME*feoAB* and pME*tonB3* plasmids, generated by cloning the *feoAB* and *tonB3* genes under control of the constitutive P*tac* promoter in the pME6031 vector (60), respectively. Additional details on the generation of *A. baumannii* mutant strains and plasmid construction are given in the supplemental material.

FURTA and β-galactosidase activity assay. The DNA fragments encompassing the putative promoter region of the *tonB1-exbB1-exbD1.1-exbD1.2, tonB2*, *tonB3-exbB3-exbD3*, and *feoABC* operons (Fig. 1) were obtained by PCR amplification with primers (no. 29 to 36) listed in Table S2 and cloned at the EcoRI-BamHI restriction sites of the pBluescript-II KS (pBS) vector to yield pBSP_{tonB1}, pBSP_{tonB2}, pBSP_{tonB3}, and pBSP_{feoA} (Table 1). These plasmids were introduced into *E. coli* H1717 to assess the FURTA phenotype, as described previously 27. Briefly, 1-ml bacterial cultures grown overnight at 37°C in LB were washed twice with saline and diluted to obtain ca. 10^8 cells/ml. Ten microliters of the resulting bacterial suspensions was spotted on MacConkey agar plates supplemented with 100 μM $FeSO_4$ (Fig. 4D) or with $FeSO_4$ concentrations ranging from 0 μM to 50 μM (see Fig. S3 in the supplemental material). Plates were incubated at 37°C for 24 h. Putative promoter regions of the *tonB1*, *tonB2*, *tonB3*, *feoA*, and *basA* genes were PCR amplified with primers listed in Table S2 and cloned in the pMP220 vector for transcriptional fusions. The resulting plasmids, namely, pMPP_{tonB1}, pMPP_{tonB2}, pMPP_{tonB3}, pMPP_{feoA}, and pMPP_{basA} (26), were independently introduced in *A. baumannii* ATCC 19606^T by electroporation, and transformants were selected on LA plates containing 50 μg/ml Tc. Promoter activities were assessed by measuring β-galactosidase (LacZ) expression levels. For this purpose, *A. baumannii* ATCC 19606^T carrying the different plasmids was grown at 37°C for 16 h in M9 with 100 μM DIP or 100 μM $FeCl_3$.

The LacZ activity was determined spectrophotometrically using *o*-nitrophenyl-β-D-galactopyranoside (ONPG) as the substrate after permeabilization of bacterial cells. Cell permeabilization was as follows: 1-ml bacterial cultures were pelleted by centrifugation and resuspended in 500 μl of sterile saline containing 250 μg/ml lysozyme, and the resulting cell suspensions were incubated for 15 min at room before addition of 30 μl lysis buffer (10% SDS, 0.02 M $MnCl_2$, toluene, and 2-β-mercaptoethanol) and subsequent incubation for 30 min at 37°C. LacZ activity is expressed as Miller units. Experiments were conducted in triplicate.

Real-time PCR analysis. Total RNA was extracted from 5-ml cultures of the parental ATCC 19606^T strain grown for 16 h at 37°C in M9 and in M9 supplemented with 100 μM $FeCl_3$ or 100 μM DIP. Briefly, bacterial cells were pelleted by centrifugation at 4,500 $\times$ *g* for 20 min, and total RNA extraction was performed using the miRNeasy minikit (Qiagen), including the on-column DNase I digestion step. Eluted RNAs were treated for 1 h at 37°C with Turbo DNase (Ambion), following the manufacturer's instructions. DNase I was removed with the RNeasy column purification kit (Qiagen). The absence of chromosomal DNA was verified by PCR with primers pairs 49 and 50 (Table S2) (61). cDNA synthesis was performed using the iScript Reverse Transcription Supermix for the reverse transcription-quantitative PCR (RT-qPCR) kit (Bio-Rad). Real-time PCRs were performed using the iTaq Universal SYBR Green Supermix (Bio-Rad) and primers 37 to 48 (Table S2). *recA* was used as the internal control to normalize the real-time PCR data and to calculate the relative fold change in gene expression by using the $2^{-\Delta\Delta CT}$ method. The analysis was performed in three technical replicates.

CAS agar assay. The ability of *A. baumannii* ATCC 19606^T and isogenic iron uptake mutants to produce iron chelators (siderophores) was investigated using the CAS agar assay (24). Briefly, 1 ml of bacterial culture grown at 37°C in LB was washed with sterile saline and diluted to obtain ca. 10^8 cells/ml. Ten microliters of this bacterial suspension was spotted on CAS agar plates and incubated for up to 48 h at 37°C. The halo around each spot provided a semiquantitative estimation of the amount of released siderophores.

Measurement of intracellular iron content. Intracellular iron content was measured according to a procedure described previously (62). Briefly, cells grown in M9 supplemented with 20 μM $FeCl_3$ were collected by centrifugation, washed twice with saline, diluted in 200 ml of M9 supplemented with 1 μM $FeCl_3$ to an optical density at 600 nm (OD_{600}) of 0.05, and incubated for 60 h at 37°C with shaking at 200 rpm. Cells were then collected by centrifugation, washed with saline, lysed in HNO_3, and analyzed by ICP-OES with an ICP-OES 710 Varian spectrometer (Agilent Technologies). In parallel, total protein content in the same cultures was evaluated by using the Coomassie protein assay reagent (Sigma-Aldrich). Iron levels determined by ICP-OES were normalized to the total protein content of each sample. Results are the means from triplicate experiments.

Assays performed in HS and in NHS. An existing stock of normal human serum (NHS) pooled from healthy donors (Policlinico Umberto I, Sapienza University of Rome) was used (28). For the growth assays in heat-inactivated human serum (HS), complement was inactivated by incubation at 56°C for 30 min, and the bulk of HS was sterilized by filtration as previously described (28) and then stored at 4°C until used. Growth of *A. baumannii* in HS was assessed in microtiter plates at 37°C with moderate shaking. Bacteria were grown overnight at 37°C in LB, washed with sterile saline, and then diluted to an OD_{600} of 0.01 in 200 μl of HS supplemented or not with 100 or 200 μM $FeCl_3$. Growth was measured spectrophotometrically (OD_{600}) in a Wallac 1420 Victor^{3V} multilabel plate reader (Perkin Elmer) at 48 h postinoculation.

Susceptibility to the bactericidal activity of NHS was assessed as previously described (63). Briefly, bacterial cells grown in 3 ml of LB for 16 h at 37°C were diluted in sterile saline to obtain ca. 1×10^7 CFU/ml. Ten microliters of bacterial suspension was added to 90 μl of freshly sampled NHS in 96-well microtiter plates. Viable cell counts were determined at different times by plating 10-fold serial dilutions (10^0 to 10^{-4}) on LB agar plates.

***In vivo* infection assays.** The *G. mellonella* larva killing assay was performed as previously described (6, 64). Bacterial cells were cultured in LB for 16 h at 37°C with shaking, collected by centrifugation, washed twice, and diluted in saline to ca. 10^8 CFU/ml. A 1-ml BD Plastipak insulin syringe with a 0.3-mm needle, mounted on a Tridak stepper pipette, was used to inject ca. 1×10^6 bacterial cells (10-μl inoculation) into the hemocoel of each caterpillar through the last left proleg. *G. mellonella* larvae were incubated at 37°C, and their viability was monitored every 24 h for 3 days. The experiment was performed twice using 15 larvae for experimental groups ($n = 30$).

Six- to 8-week-old specific-pathogen-free female BALB/c mice were purchased from Charles Rivers Laboratories (St. Constant, QC, Canada). The mice were housed and used in accordance with the recommendations of the Canadian Council on Animal Care Guide to the Care and Use of Experimental Animals. This study and all animal care/use protocols were approved (AUP no. 2012.12) by the Human Health Therapeutics Animal Care Committee (HHT-ACC), National Research Council of Canada.

Fresh inocula were prepared for each experiment from the frozen stocks of *A. baumannii* ATCC 19606^T and derivative mutants, as previously described (65). Briefly, bacteria were grown overnight on cysteine heart agar (CHA) plates, and a portion was transferred into brain heart infusion broth and incubated at 37°C at 200 rpm for 3 to 4 h until an OD_{600} of 0.85 was reached. Bacterial cells were then centrifuged and suspended in 0.85% saline at 10× the desired inoculation concentration. Immediately before the inoculation, the bacteria were further diluted 1:10 in 5% porcine mucin (Sigma-Aldrich), in order to obtain a final inoculum of 10^4 to 10^6 CFU per mouse (31). The inoculum concentration was confirmed by plate counting. Groups of mice were intraperitoneally (i.p.) inoculated with 10^4 to 10^6 CFU of different *A. baumannii* strains in 0.5 ml, and clinical signs and survival were observed and recorded once or twice daily for 5 days.

Statistical analysis. Statistical analysis was performed with the GraphPad Instat software. For the NHS assay, comparisons between groups were performed using the Student *t* test. Survival curves for the *G. mellonella* and mouse killing assays were generated by the Kaplan-Meier method and analyzed by the log rank test. Differences having a *P* value of ≤ 0.05 were considered statistically significant.

SUPPLEMENTAL MATERIAL

Supplemental material for this article may be found at https://doi.org/10.1128/IAI.00755-18.

SUPPLEMENTAL FILE 1, PDF file, 4.3 MB.

ACKNOWLEDGMENTS

We thank the personnel at Policlinico Umberto I, Sapienza University of Rome, for help in collecting serum samples from healthy donors. We also thank Alessia Falsetti (Tor Vergata University of Rome) for performing the ICP-OES measurements.

The Grant of Excellence Departments, MIUR-Italy (ARTICOLO 1, COMMI 314-337 LEGGE 232/2016), is gratefully acknowledged. The work of J.S. and B.A. was supported by a grant from the Deutsche Forschungsgemeinschaft through DFG Research Unit FOR 2251.

The funders had no role in study design, data collection and interpretation, or the decision to submit the work for publication.

REFERENCES

1. Peleg AY, Jara S, Monga D, Eliopoulos GM, Moellering RC, Jr, Mylonakis E. 2009. *Galleria mellonella* as a model system to study *Acinetobacter baumannii* pathogenesis and therapeutics. Antimicrob Agents Chemother 53:2605–2609. https://doi.org/10.1128/AAC.01533-08.
2. Crosa JH, Mey AR, Payne SM. 2004. Iron transport in bacteria. ASM Press, Washington, DC.
3. Wandersman C, Stojiljkovic I. 2000. Bacterial heme sources: the role of heme, hemoprotein receptors and hemophores. Curr Opin Microbiol 3:215–220. https://doi.org/10.1016/S1369-5274(00)00078-3.
4. Gaddy JA, Arivett BA, McConnell MJ, López-Rojas R, Pachón J, Actis LA. 2012. Role of acinetobactin-mediated iron acquisition functions in the interaction of *Acinetobacter baumannii* strain ATCC 19606^T with human lung epithelial cells, *Galleria mellonella* caterpillars, and mice. Infect Immun 80:1015–1024. https://doi.org/10.1128/IAI.06279-11.
5. Mortensen BL, Skaar EP. 2013. The contribution of nutrient metal acquisition and metabolism to *Acinetobacter baumannii* survival within the host. Front Cell Infect Microbiol 3:95. https://doi.org/10.3389/fcimb.2013.00095.
6. Zimbler DL, Arivett BA, Beckett AC, Menke SM, Actis LA. 2013. Functional features of TonB energy transduction systems of *Acinetobacter baumannii*. Infect Immun 81:3382–3394. https://doi.org/10.1128/IAI.00540-13.
7. Ratledge C, Dover LG. 2000. Iron metabolism in pathogenic bacteria. Annu Rev Microbiol 54:881–941. https://doi.org/10.1146/annurev.micro.54.1.881.
8. Antunes LC, Imperi F, Towner KJ, Visca P. 2011. Genome-assisted identification of putative iron-utilization genes in *Acinetobacter baumannii* and their distribution among a genotypically diverse collection of clinical isolates. Res Microbiol 162:279–284. https://doi.org/10.1016/j.resmic.2010.10.010.
9. Fillat MF. 2014. The FUR (ferric uptake regulator) superfamily: diversity and versatility of key transcriptional regulators. Arch Biochem Biophys 546:41–52. https://doi.org/10.1016/j.abb.2014.01.029.
10. Cartron ML, Maddocks S, Gillingham P, Craven CJ, Andrews SC. 2006. Feo-transport of ferrous iron into bacteria. Biometals 19:143–157. https://doi.org/10.1007/s10534-006-0003-2.
11. Lau CK, Krewulak KD, Vogel HJ. 2016. Bacterial ferrous iron transport: the Feo system. FEMS Microbiol Rev 40:273–298. https://doi.org/10.1093/femsre/fuv049.
12. Noinaj N, Guillier M, Barnard TJ, Buchanan SK. 2010. TonB-dependent transporters: regulation, structure, and function. Annu Rev Microbiol 64:43–60. https://doi.org/10.1146/annurev.micro.112408.134247.
13. Postle K, Kadner RJ. 2003. Touch and go: tying TonB to transport. Mol Microbiol 49:869–882. https://doi.org/10.1046/j.1365-2958.2003.03629.x.
14. Klebba PE. 2016. ROSET model of TonB action in Gram-negative bacterial iron acquisition. J Bacteriol 198:1013–1021. https://doi.org/10.1128/JB.00823-15.
15. Krewulak KD, Vogel HJ. 2011. TonB or not TonB: is that the question? Biochem Cell Biol 89:87–97. https://doi.org/10.1139/o10-141.
16. Postle K, Larsen RA. 2007. TonB-dependent energy transduction between outer and cytoplasmic membranes. Biometals 20:453–465. https://doi.org/10.1007/s10534-006-9071-6.
17. Poole K, Zhao Q, Neshat S, Heinrichs DE, Dean CR. 1996. The *Pseudomonas aeruginosa tonB* gene encodes a novel TonB protein. Microbiology 142:1449–1458. https://doi.org/10.1099/13500872-142-6-1449.
18. Higgs PI, Myers PS, Postle K. 1998. Interactions in the TonB-dependent energy transduction complex: ExbB and ExbD form homomultimers. J Bacteriol 180:6031–6038.
19. Zhao Q, Poole K. 2002. Mutational analysis of the TonB1 energy coupler of *Pseudomonas aeruginosa*. J Bacteriol 184:1503–1513. https://doi.org/10.1128/JB.184.6.1503-1513.2002.
20. Marshall B, Stintzi A, Gilmour C, Meyer JM, Poole K. 2009. Citrate-mediated iron-uptake in *Pseudomonas aeruginosa*: involvement of the citrate-inducible FecA receptor and the FeoB ferrous iron transporter. Microbiology 155:305–315. https://doi.org/10.1099/mic.0.023531-0.
21. Minandri F, Imperi F, Frangipani E, Bonchi C, Visaggio D, Facchini M, Pasquali P, Bragonzi A, Visca P. 2016. Role of iron-uptake systems in *Pseudomonas aeruginosa* virulence and airway infection. Infect Immun 84:2324–2335. https://doi.org/10.1128/IAI.00098-16.
22. Stahl J, Bergmann H, Göttig S, Ebersberger I, Averhoff B. 2015. *Acinetobacter baumannii* virulence is mediated by the concerted action of three phospholipases D. PLoS One 10:e0138360. https://doi.org/10.1371/journal.pone.0138360.
23. Llamas MA, Imperi F, Visca P, Lamont IL. 2014. Cell-surface signaling in *Pseudomonas*: stress responses, iron transport, and pathogenicity. FEMS Microbiol Rev 38:569–597. https://doi.org/10.1111/1574-6976.12078.
24. Schwyn B, Neilands JB. 1987. Universal chemical assay for the detection and determination of siderophores. Anal Biochem 160:47–56. https://doi.org/10.1016/0003-2697(87)90612-9.
25. Solovyev V, Salamov A. 2011. Automatic annotation of microbial genomes and metagenomic sequences, p 61–78. *In* Li RW (ed), Metagenomics and its applications in agriculture, biomedicine and environmental studies. Nova Science Publishers, Hauppauge, NY.
26. Antunes LC, Imperi F, Minandri F, Visca P. 2012. *In vitro* and *in vivo* antimicrobial activities of gallium nitrate against multidrug-resistant *Acinetobacter baumannii*. Antimicrob Agents Chemother 56:5961–5970. https://doi.org/10.1128/AAC.01519-12.
27. Stojiljkovic I, Bäumler AJ, Hantke K. 1994. Fur regulon in gram-negative bacteria. Identification and characterization of new iron-regulated *Escherichia coli* genes by a fur titration assay. J Mol Biol 236:531–545. https://doi.org/10.1006/jmbi.1994.1163.
28. Runci F, Bonchi C, Frangipani E, Visaggio D, Visca P. 2016. *Acinetobacter baumannii* biofilm formation in human serum and disruption by gallium. Antimicrob Agents Chemother 61:e01563-16. https://doi.org/10.1128/AAC.01563-16.
29. Harding CM, Hennon SW, Feldman MF. 2018. Uncovering the mechanisms of *Acinetobacter baumannii* virulence. Nat Rev Microbiol 16:91–102. https://doi.org/10.1038/nrmicro.2017.148.
30. Gebhardt MJ, Gallagher LA, Jacobson RK, Usacheva EA, Peterson LR, Zurawski DV, Shuman HA. 2015. Joint transcriptional control of virulence and resistance to antibiotic and environmental stress in *Acinetobacter baumannii*. mBio 6:e01660-15. https://doi.org/10.1128/mBio.01660-15.
31. McConnell MJ, Pachón J. 2010. Active and passive immunization against *Acinetobacter baumannii* using an inactivated whole cell vaccine. Vaccine 29:1–5. https://doi.org/10.1016/j.vaccine.2010.10.052.
32. Cassat JE, Skaar EP. 2013. Iron in infection and immunity. Cell Host Microbe 13:509–519. https://doi.org/10.1016/j.chom.2013.04.010.
33. Stojiljkovic I, Cobeljic M, Hantke K. 1993. *Escherichia coli* K-12 ferrous iron-uptake mutants are impaired in their ability to colonize the mouse intestine. FEMS Microbiol Lett 108:111–115. https://doi.org/10.1111/j.1574-6968.1993.tb06082.x.
34. Velayudhan J, Hughes NJ, McColm AA, Bagshaw J, Clayton CL, Andrews SC, Kelly DJ. 2000. Iron acquisition and virulence in *Helicobacter pylori*: a major role for FeoB, a high-affinity ferrous iron transporter. Mol Microbiol 37:274–286. https://doi.org/10.1046/j.1365-2958.2000.01987.x.
35. Awad MM, Cheung JK, Tan JE, McEwan AG, Lyras D, Rood JI. 2016. Functional analysis of a *feoB* mutant in *Clostridium perfringens* strain 13. Anaerobe 41:10–17. https://doi.org/10.1016/j.anaerobe.2016.05.005.
36. Subashchandrabose S, Smith S, DeOrnellas V, Crepin S, Kole M, Zahdeh C, Mobley HL. 2015. *Acinetobacter baumannii* genes required for bacterial survival during bloodstream infection. mSphere 1:e00013-15. https://doi.org/10.1128/mSphere.00013-15.
37. Grupper M, Sprecher H, Mashiach T, Finkelstein R. 2007. Attributable mortality of nosocomial *Acinetobacter* bacteremia. Infect Control Hosp Epidemiol 28:293–298. https://doi.org/10.1086/512629.
38. Seliger SS, Mey AR, Valle AM, Payne SM. 2001. The two TonB systems of *Vibrio cholerae*: redundant and specific functions. Mol Microbiol 39:801–812. https://doi.org/10.1046/j.1365-2958.2001.02273.x.
39. Stork M, Di Lorenzo M, Mouriño S, Osorio CR, Lemos ML, Crosa JH. 2004. Two *tonB* systems function in iron transport in *Vibrio anguillarum*, but only one is essential for virulence. Infect Immun 72:7326–7329. https://doi.org/10.1128/IAI.72.12.7326-7329.2004.
40. Chu BC, Peacock RS, Vogel HJ. 2007. Bioinformatic analysis of the TonB protein family. Biometals 20:467–483. https://doi.org/10.1007/s10534-006-9049-4.
41. Heller K, Kadner RJ. 1985. Nucleotide sequence of the gene for the vitamin B12 receptor protein in the outer membrane of *Escherichia coli*. J Bacteriol 161:904–908.
42. Eick-Helmerich K, Braun V. 1989. Import of biopolymers into *Escherichia coli*: nucleotide sequences of the *exbB* and *exbD* genes are homologous to those of the *tolQ* and *tolR* genes, respectively. J Bacteriol 171:5117–5126. https://doi.org/10.1128/jb.171.9.5117-5126.1989.

43. Jarosik GP, Sanders JD, Cope LD, Muller-Eberhard U, Hansen EJ. 1994. A functional *tonB* gene is required for both utilization of heme and virulence expression by *Haemophilus influenzae* type b. Infect Immun 62:2470–2477.
44. Huang B, Ru K, Yuan Z, Whitchurch CB, Mattick JS. 2004. *tonB3* is required for normal twitching motility and extracellular assembly of type IV pili. J Bacteriol 186:4387–4389. https://doi.org/10.1128/JB.186.13.4387-4389.2004.
45. Dorsey CW, Tomaras AP, Connerly PL, Tolmasky ME, Crosa JH, Actis LA. 2004. The siderophore-mediated iron acquisition systems of *Acinetobacter baumannii* ATCC19606 and *Vibrio anguillarum* 775 are structurally and functionally related. Microbiology 150:3657–3667. https://doi.org/10.1099/mic.0.27371-0.
46. Mihara K, Tanabe T, Yamakawa Y, Funahashi T, Nakao H, Narimatsu S, Yamamoto S. 2004. Identification and transcriptional organization of a gene cluster involved in biosynthesis and transport of acinetobactin, a siderophore produced by *Acinetobacter baumannii* ATCC19606^T. Microbiology 150:2587–2597. https://doi.org/10.1099/mic.0.27141-0.
47. Eijkelkamp BA, Hassan KA, Paulsen IT, Brown MH. 2011. Investigation of the human pathogen *Acinetobacter baumannii* under iron limiting conditions. BMC Genomics 12:126. https://doi.org/10.1186/1471-2164-12-126.
48. Torres AG, Redford P, Welch RA, Payne SM. 2001. TonB-dependent systems of uropathogenic *Escherichia coli*: aerobactin and heme transport and TonB are required for virulence in the mouse. Infect Immun 69:6179–6185. https://doi.org/10.1128/IAI.69.10.6179-6185.2001.
49. Beddek AJ, Sheehan BJ, Bossé JT, Rycroft AN, Kroll JS, Langford PR. 2004. Two TonB systems in *Actinobacillus pleuropneumoniae*: their roles in iron acquisition and virulence. Infect Immun 72:701–708. https://doi.org/10.1128/IAI.72.2.701-708.2004.
50. Alvarez B, Alvarez J, Menéndez A, Guijarro JA. 2008. A mutant in one of two *exbD* loci of a TonB system in *Flavobacterium psychrophilum* shows attenuated virulence and confers protection against cold water disease. Microbiology 154:1144–1151. https://doi.org/10.1099/mic.0.2007/010900-0.
51. Hsieh PF, Lin TL, Lee CZ, Tsai SF, Wang JT. 2008. Serum-induced iron-acquisition systems and TonB contribute to virulence in *Klebsiella pneumoniae* causing primary pyogenic liver abscess. J Infect Dis 197:1717–1727. https://doi.org/10.1086/588383.
52. Foley TL, Simeonov A. 2012. Targeting iron assimilation to develop new antibacterials. Expert Opin Drug Discov 7:831–847. https://doi.org/10.1517/17460441.2012.708335.
53. Ferreira D, Seca AM, C G A D, Silva AM. 2016. Targeting human pathogenic bacteria by siderophores: a proteomics review. J Proteomics 145:153–166. https://doi.org/10.1016/j.jprot.2016.04.006.
54. Yep A, McQuade T, Kirchhoff P, Larsen M, Mobley HL. 2014. Inhibitors of TonB function identified by a high-throughput screen for inhibitors of iron acquisition in uropathogenic *Escherichia coli* CFT073. mBio 5:e01089-13. https://doi.org/10.1128/mBio.01089-13.
55. Nairn BL, Eliasson OS, Hyder DR, Long NJ, Majumdar A, Chakravorty S, McDonald P, Roy A, Newton SM, Klebba PE. 2017. Fluorescence high-throughput screening for inhibitors of TonB action. J Bacteriol 199:e00889-16. https://doi.org/10.1128/JB.00889-16.
56. Murray GL, Tsyganov K, Kostoulias XP, Bulach DM, Powell D, Creek DJ, Boyce JD, Paulsen IT, Peleg AY. 2017. Global gene expression profile of *Acinetobacter baumannii* during bacteremia. J Infect Dis 215:S52–S57. https://doi.org/10.1093/infdis/jiw529.
57. Mott TM, Vijayakumar S, Sbrana E, Endsley JJ, Torres AG. 2015. Characterization of the *Burkholderia mallei tonB* mutant and its potential as a backbone strain for vaccine development. PLoS Negl Trop Dis 9:e0003863. https://doi.org/10.1371/journal.pntd.0003863.
58. Pradenas GA, Myers JN, Torres AG. 2017. Characterization of the *Burkholderia cenocepacia* TonB mutant as a potential live attenuated vaccine. Vaccines (Basel) 5:E33. https://doi.org/10.3390/vaccines5040033.
59. Sambrook J, Fritsch EF, Maniatis T. 1989. Molecular cloning: a laboratory manual, 2nd ed. Cold Spring Harbor Laboratory Press, Cold Spring Harbor, NY.
60. Heeb S, Itoh Y, Nishijyo T, Schnider U, Keel C, Wade J, Walsh U, O'Gara F, Haas D. 2000. Small, stable shuttle vectors based on the minimal pVS1 replicon for use in Gram-negative, plant-associated bacteria. Mol Plant-Microbe Interact 13:232–237. https://doi.org/10.1094/MPMI.2000.13.2.232.
61. Lucidi M, Runci F, Rampioni G, Frangipani E, Leoni L, Visca P. 2018. New shuttle vectors for gene cloning and expression in multidrug-resistant *Acinetobacter* species. Antimicrob Agents Chemother 62:e02480-17. https://doi.org/10.1128/AAC.02480-17.
62. Pasqua M, Visaggio D, Lo Sciuto A, Genah S, Banin E, Visca P, Imperi F. 2017. Ferric uptake regulator Fur is conditionally essential in Pseudomonas aeruginosa. J Bacteriol 199:e00472-17. https://doi.org/10.1128/JB.00472-17.
63. Kim SW, Choi CH, Moon DC, Jin JS, Lee JH, Shin JH, Kim JM, Lee YC, Seol SY, Cho DT, Lee JC. 2009. Serum resistance of *Acinetobacter baumannii* through the binding of factor H to outer membrane proteins. FEMS Microbiol Lett 301:224–231. https://doi.org/10.1111/j.1574-6968.2009.01820.x.
64. Peleg AY, Seifert H, Paterson DL. 2008. *Acinetobacter baumannii*: emergence of a successful pathogen. Clin Microbiol Rev 21:538–582. https://doi.org/10.1128/CMR.00058-07.
65. van Faassen H, KuoLee R, Harris G, Zhao X, Conlan JW, Chen W. 2007. Neutrophils play an important role in host resistance to respiratory infection with *Acinetobacter baumannii* in mice. Infect Immun 75:5597–5608. https://doi.org/10.1128/IAI.00762-07.
66. Harley CB, Reynolds RP. 1987. Analysis of *E. coli* promoter sequences. Nucleic Acids Res 15:2343–2361. https://doi.org/10.1093/nar/15.5.2343.
67. Spaink HP, Okker RJ, Wijffelman CA, Pees E, Lugtenberg BJ. 1987. Promoters in the nodulation region of the *Rhizobium leguminosarum* Sym plasmid pRL1JI. Plant Mol Biol 9:27–39. https://doi.org/10.1007/BF00017984.